A Comparative Analysis of 7.0-Tesla Magnetic Resonance Imaging and Histology Measurements of Knee Articular Cartilage in a Canine Posterolateral Knee Injury Model

A Preliminary Analysis

Scott R. Pepin,* MD, Chad J. Griffith,* MD, Coen A. Wijdicks,* MSc, Ute Goerke,† PhD, Margaret A. McNulty,‡ Josh B. Parker, BS, Cathy S. Carlson,‡ DVM, PhD, Jutta Ellermann,† MD, PhD, and Robert F. LaPrade,*§ MD, PhD
*From the *Orthopaedic Biomechanics Laboratory, Department of Orthopaedic Surgery, †Center for Magnetic Resonance Imaging—Department of Radiology, and ‡Department of Veterinary Population Medicine, University of Minnesota, Minneapolis, Minnesota*

Background: There has recently been increased interest in the use of 7.0-T magnetic resonance imaging for evaluating articular cartilage degeneration and quantifying the progression of osteoarthritis.

Purpose: The purpose of this study was to evaluate articular cartilage cross-sectional area and maximum thickness in the medial compartment of intact and destabilized canine knees using 7.0-T magnetic resonance images and compare these results with those obtained from the corresponding histologic sections.

Study Design: Controlled laboratory study.

Methods: Five canines had a surgically created unilateral grade III posterolateral knee injury that was followed for 6 months before euthanasia. The opposite, noninjured knee was used as a control. At necropsy, 3-dimensional gradient echo images of the medial tibial plateau of both knees were obtained using a 7.0-T magnetic resonance imaging scanner. Articular cartilage area and maximum thickness in this site were digitally measured on the magnetic resonance images. The proximal tibias were processed for routine histologic analysis with hematoxylin and eosin staining. Articular cartilage area and maximum thickness were measured in histologic sections corresponding to the sites of the magnetic resonance slices.

Results: The magnetic resonance imaging results revealed an increase in articular cartilage area and maximum thickness in surgical knees compared with control knees in all specimens; these changes were significant for both parameters ($P < .05$ for area; $P < .01$ for thickness). The average increase in area was 14.8% and the average increase in maximum thickness was 15.1%. The histologic results revealed an average increase in area of 27.4% ($P < .05$) and an average increase in maximum thickness of 33.0% ($P = .06$). Correlation analysis between the magnetic resonance imaging and histology data revealed that the area values were significantly correlated ($P < .01$), but the values for thickness obtained from magnetic resonance imaging were not significantly different from the histology sections ($P > .1$).

Conclusion: These results demonstrate that 7.0-T magnetic resonance imaging provides an alternative method to histology to evaluate early osteoarthritic changes in articular cartilage in a canine model by detecting increases in articular cartilage area.

Clinical Relevance: The noninvasive nature of 7.0-T magnetic resonance imaging will allow for in vivo monitoring of osteoarthritis progression and intervention in animal models and humans for osteoarthritis.

Keywords: 7-T magnetic resonance imaging (MRI); histology; osteoarthritis; posterolateral knee; articular cartilage area

§Address correspondence to Robert F. LaPrade, MD, PhD, Professor, Sports Medicine and Shoulder Surgery, Director, University of Minnesota Orthopaedic Biomechanics Laboratory, Department of Orthopaedic Surgery, University of Minnesota, 2450 Riverside Avenue South, R200, Minneapolis, MN 55454 (e-mail: lapra001@umn.edu).

No potential conflict of interest declared.

The American Journal of Sports Medicine, Vol. 37, Supplement 1
DOI: 10.1177/0363546509350439

Recent studies have focused on the evaluation of articular cartilage with ultra-high–field 7.0-T MRI.[4,11,18,28-30,32,33] Interest in the use of 7.0-T MRI for analyzing articular cartilage and quantifying the early progression of osteoarthritis is based on the fact that the signal-to-noise ratio increases linearly with magnetic field strength. Because the signal-to-noise is also proportional to the size of a voxel (referring to a volume element in analogy to a pixel in a digital image), a higher spatial resolution can be achieved at increased magnetic field strength for the same signal-to-noise ratio and total imaging time compared with clinical field strengths of 1.5 T and 3.0 T.[4,28] The improved resolution at 7.0 T reportedly allows for improved visualization of articular cartilage[28] and for quantitative and qualitative evaluations of this tissue.[11,33] The objective of our approach was to investigate whether the subtle anatomic changes caused by early osteoarthritis can be detected with high-resolution MRI at ultra-high magnetic field strength. The imaging parameters were optimized on a 7.0-T human scanner with the goal that these protocols will be used for in vivo studies in canine models and humans in the future.

Our hypothesis was that 7.0-T high-field MRI would yield comparable information to histologic sections regarding articular cartilage areas and maximum thicknesses. In this study, the articular cartilage area and thickness were used as markers because they were expected to increase in the early stages of osteoarthritis.[25] Our purpose was to quantify articular cartilage cross-sectional area and thickness in the medial tibial plateau in unoperated and surgically destabilized canine knee joints 6 months after unilateral posterolateral knee injury using 7.0-T magnetic resonance images and to compare these results with the same measurements made in the corresponding histologic sections. The canine model was chosen because it provides a large enough model for future surgical reconstruction studies and because it provides an instability model that was more similar to the human knee than the previously described goat model.[14,21,22,27] The posterolateral knee model also provides an injury model with a slower progression of osteoarthritis than previous models,[27] which allows for the ability to determine how future treatment affects its potential progression. Validating the 7.0-T MRI results by demonstrating a correlation with histologic results would allow for improved in vivo assessments of these changes in a canine model and, potentially, in human disease.

MATERIALS AND METHODS

Posterolateral Knee In Vivo Injury Model

Five skeletally mature, adult male, mixed-breed canines were used for this particular study. Approval for the study was obtained from the Institutional Animal Care and Use Committee at the University of Minnesota.

A simulated posterolateral knee injury was created using a previously described model[14] by placing a Kirschner wire medial (deep) to the fibular collateral ligament. Several small longitudinal stab incisions were made in the ligament and brisk lateral traction resulted in a mid-substance mop-end tear of the fibular collateral ligament; these ends were left in situ.[14,21,22,33] Similarly, the popliteus tendon and popliteofibular ligament were exposed and ruptured. Hemostasis was obtained and the skin was closed with a subcuticular stitch. No metallic hardware, such as the Kirschner wire, remained in the tissue. The canines were housed individually in 4- × 6-foot pens, were fed commercial dog food, had ad libitum access to water, and were exercised twice daily.

Specimen Preparation

Humane euthanasia was performed 6 months after the surgical procedure, and both hindlimbs were disarticulated at the hip joint. Both knees from each canine were prepared for immediate MRI and later histologic evaluation by severing the thigh at the midfemur and the leg at the distal tibia. All soft tissues surrounding the knee were retained during the MRI scans.

Magnetic Resonance Imaging Technique

Three-Dimensional Gradient Echo Image Acquisition. The knees were placed in full extension (mean, 28.5° of knee flexion; range, 24°-35°) in the MRI scanner. The MRI scout films were used to confirm that the knees were parallel to the long axis of the tibia to verify that the slices were being acquired directly perpendicular to the articular cartilage surfaces of the medial tibial plateau. Three-dimensional gradient echo (3D GRE) images were acquired with a 7.0-T scanner (Siemens, Erlangen, Germany) with a 90-cm bore and 4-G/cm gradient strength. A quadrature surface coil with separate receive and transmit channels was used. A 3D GRE sequence with an isotropic resolution of 310 μm was used, which provided a sufficient signal-to-noise ratio for measuring the cartilage thickness and area with the necessary accuracy. Relaxation time and echo time settings were adjusted for optimal signal-to-noise, coverage of the joint, and total imaging time. The animal model of posterolateral corner injury was done without permanent metallic hardware; therefore, susceptibility artifacts were not present. To avoid chemical shift artifact of the fat signal from the marrow in the trabecular bone, that is, the displacement relative to the readout direction of the signal originating from fatty tissue, at the subchondral bone cartilage interface in the coronal plane, the readout gradient was oriented along the left-to-right direction of the joint. Hence, an overlap of signal of the cartilage and displaced signal originating from the marrow was avoided. The imaging parameters were acquired matrix size 384 × 288 × 192, from which a final matrix size of 384 × 384 × 256 was obtained using partial Fourier reconstruction in the slice and the phase-encoded dimension; echo time, 5.1 milliseconds; repetition time, 16 milliseconds; one average, isotropic resolution 310 μm; and acquisition bandwidth, 320 Hz/pixel, with a total imaging time of approximately 15 minutes. These

imaging parameters are typical for in vivo anatomic imaging of joints in humans at 7 T.[5,9,29]

Analysis of MRI Measurements. The magnetic resonance images were viewed with iQ-View 2.5.0 (IMAGE Information Systems Ltd, London, United Kingdom). Landmarks were identified both on the microradiographs of the 4-mm–thick serial coronal slabs of the medial tibial plateau and the histologic sections from these sites (details provided below). The equivalent MRI slices based on matching landmarks to the histologic sections were measured. Images were observed in their original contrast settings, as well as an inverted contrast setting to allow for the ability to discern the articular cartilage-subchondral bone junction (Figure 1). In addition, measurements were made of the femoral condyle width and notch height for scaling with the iQ-View measurement tool.

Images were then exported to Adobe Photoshop (Adobe Systems Inc, San Jose, California), where pixel dimensions were standardized with known condyle and notch measurements from the magnetic resonance images measured with the iQ-View measurement tool. This was done by dividing the medial femoral condyle and notch dimensions from iQ-View by the pixel count measurement in Adobe Photoshop. The images were then relabeled, randomized, and measured in a randomized fashion. The area of the articular cartilage of the medial tibial plateau was measured next by outlining the entire visualized articular cartilage area in the single coronal image (Figure 1). The number of pixels outlined was then multiplied by the pixel area to determine the articular cartilage area. Next, the thickness of the articular cartilage was measured at the superior edge of maximal thickness, using a line drawn from the articular surface to the site of the subchondral bone perpendicular to the chondroosseous junction. The thickness in pixels was then converted to millimeters by multiplying by pixel length. The measurements were performed 6 times for each knee and averaged.

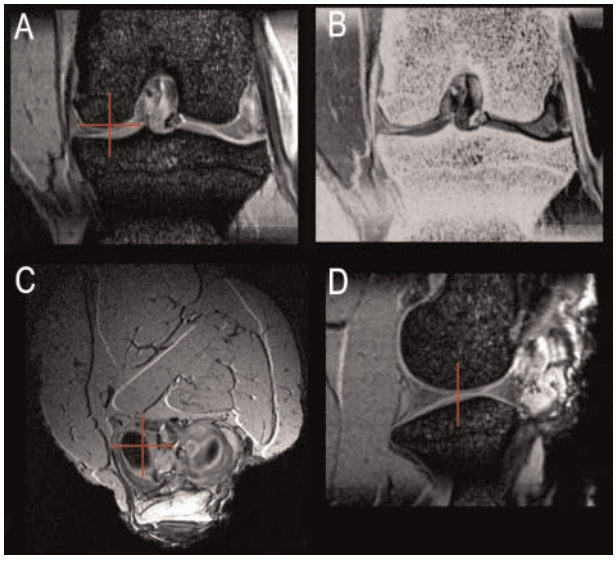

Figure 1. Representative outline of medial tibial plateau articular cartilage that was measured on magnetic resonance images, with normal (A) and inverted (B) contrast. The analogous axial (C) and sagittal (D) MRI views used to help localize the coronal slice on the magnetic resonance image are also shown.

Histologic Technique

After MRI of both the operated and control knees, the specimens were fixed in 10% neutral-buffered formalin, and each proximal tibia was serially sectioned in the coronal plane at 4-mm increments using a diamond saw (Allied High Tech Products, Inc, Racho Dominguez, California). The serial sections were then radiographed using a cabinet radiography unit (Faxitron series, Hewlett Packard, McMinnville, Oregon). The technique included 45 kVp exposure, mAs of 3 mA continuous for 30 seconds, and a film-to-source distance of 61 cm. Histologic sections were taken from the midcoronal region of each proximal tibia, decalcified in 10% ethylenediamine tetraacetic acid, and processed for histology. Routine paraffin-embedded specimens were sectioned at 4 μm and stained with hematoxylin and eosin (Figure 2). All histologic sections were then randomized, relabeled, and measured in a blinded fashion.

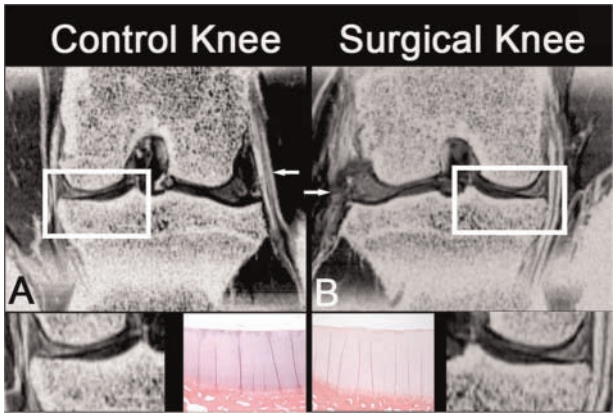

Figure 2. Representative MRIs and histology sections of the medial tibial plateau from a single canine, with A being the control knee and B being the surgical knee. White arrows refer to the intact (A) and surgically sectioned (B) fibular collateral ligament.

Histologic Area and Thickness Measurements. Articular cartilage area and maximum articular cartilage thickness of the medial tibial plateau from each stifle joint were evaluated using OsteoMeasure histomorphometry software (OsteoMetrics Inc, Decatur, Georgia). Articular cartilage area was calculated by the program from measurements of the superficial and deep perimeters of articular cartilage that were taken on 2 separate serial histologic sections and averaged. Articular cartilage thickness was measured in 1 section from the medial tibial plateau using SPOT software (Diagnostic Instruments, Inc, Sterling Heights, Michigan) by dropping a line from the articular cartilage surface to

TABLE 1
MRI Versus Histology: Articular Cartilage Area and Thickness of Medial Tibial Plateau[a]

Group	Specimen #	Articular Cartilage Area (mm^2)			Articular Cartilage Maximum Thickness (mm)		
		Knee With Intact Posterolateral Structures	Knee With Sectioned Posterolateral Structures	Percentage Change $(\frac{Sectioned-Intact}{Intact})$	Knee With Intact Posterolateral Structures	Knee With Sectioned Posterolateral Structures	Percentage Change $(\frac{Sectioned-Intact}{Intact})$
MRI	1	13.17	15.81	20.0	1.67	1.81	8.7
	2	12.93	13.17	1.9	1.39	1.67	19.4
	3	18.92	20.37	7.6	1.81	1.96	8.2
	4	11.75	14.73	25.4	1.40	1.73	24.0
	5	13.96	16.59	18.9	1.46	1.69	15.2
Mean ± SD		14.15 ± 2.78	16.30 ± 2.69[b]	14.8 ± 9.7	1.55 ± 0.18	1.77 ± 0.12[c]	15.1 ± 6.9
Histology	1	12.87	16.09	25.0	1.60	2.00	25.0
	2	17.09	16.55	−3.1	1.63	1.95	19.6
	3	18.65	23.10	23.8	2.00	2.30	15.0
	4	11.58	15.51	34.0	1.80	1.90	5.6
	5	13.94	21.92	57.3	1.40	2.80	100
Mean ± SD		14.83 ± 2.95	18.63 ± 3.58[b]	27.4 ± 21.7	1.69 ± 0.23	2.19 ± 0.37	33.0 ± 38.1

[a]SD, standard deviation.
[b]$P < .05$ compared with intact knee.
[c]$P < .01$ compared with intact knee.

a perpendicular point along the most superficial tidemark. Several measurements were taken in regions of the articular cartilage that appeared to be the thickest and, from those, the maximum thickness was recorded.

Statistical Analysis

The data were analyzed using correlation analysis (for comparison of MRI and histologic measurements) and a 2-tailed Student t test (for treatment effects on cartilage area and thickness). Statistical significance was set at $P < .05$.

RESULTS

Area and Thickness

The MRI measurements of articular cartilage area and maximum thickness of the medial tibial plateaus in the sectioned planes revealed increases in both parameters in the operative knees compared with the control knees (Table 1). The mean articular cartilage area of the intact knees (14.15 ± 2.78 mm^2) was significantly lower than the mean articular cartilage area of the operative knees (16.30 ± 2.69 mm^2; $P < .05$; 2-tailed paired t test). Similarly, the mean maximum articular cartilage thickness of the intact knees (1.55 ± 0.18 mm) was significantly lower than the mean maximum articular cartilage thickness of the operative knees (1.77 ± 0.12 mm; $P < .01$). The average percentage change in area between the 2 groups was 14.8% (range, 1.9%-25.4%; $P < .001$), and the average percentage change in maximum thickness was 15.1% (range, 8.2%-24.0%; $P < .001$).

Evaluation of the histologic sections also revealed increases in articular cartilage area and maximum thickness in the operative knees versus the control knees (Table 1). The mean articular cartilage area of the intact knees (14.83 ± 2.95 mm^2) was significantly lower than the mean articular cartilage area of the operative knees (18.63 ± 3.58 mm^2; $P < .05$; 2-tailed paired t test). Although the mean maximum articular cartilage thickness of the intact knees (1.69 ± 0.23 mm) was lower than the mean maximum articular cartilage thickness of the operative knees (2.19 ± 0.37 mm), this difference was not significant ($P = .06$). The percentage increase in area averaged 27.4% (range, −3.1%-57.3%; $P < .01$), and percentage increase in thickness averaged 33.0% (range, 5.6%-100.0%).

Magnetic Resonance Imaging Versus Histology Assessments

Correlation analysis comparing the MRI and histology data revealed that the cross-sectional area data obtained using these 2 modalities were significantly correlated ($P < .01$), with some measurements being nearly identical, particularly in the control knees. Although increases in articular cartilage thickness were seen in all operative dog knees compared with the contralateral control, correlation analysis between MRI and histology data revealed no significant correlation for the maximum thickness measurements ($P > .1$).

DISCUSSION

This study focused on comparison of MRI and histologic measurements of articular cartilage area and maximum

thickness in the intact knee versus the surgically destabilized contralateral knee 6 months after posterolateral knee destabilization surgery in a canine model. The results indicated that the cross-sectional area of articular cartilage measured on 7.0-T magnetic resonance images correlated well with area measurements in closely matched histologic sections of these same canine knees. Thus, it appears that there is potential for monitoring the effects of nonsurgical or surgical osteoarthritis interventions using high-field 7.0-T MRI techniques without the need to euthanize animals or to perform second-look arthroscopies and/or biopsies in humans to evaluate the potential progression of osteoarthritis.

We speculate that the increase in articular cartilage area and thickness that was detected using both modalities may reflect early osteoarthritic changes in this in vivo posterolateral injury canine model. In the early development of osteoarthritis, the proteoglycan concentration in the articular cartilage initially decreases, and this change has been reported to be accompanied by an increase in water content and wet weight.[1-3,6,8,12,13,23,25,26] Previous studies theorized that the increase in water content may be due to a loosening of the collagen matrix of the articular cartilage[13,23] and is associated with a change in content and organization of type II collagen and proteoglycans.[26] Increases in water content have also been reported to be accompanied by chondrocyte hypertrophy,[2,3] resulting in an increase in articular cartilage thickness by as much as 2 times,[3,25] and, in turn, articular cartilage area. Detecting osteoarthritis changes in these early stages allows for the potential to measure the effectiveness of potential early treatments to prevent more severe cartilage damage.

With the increased use of MRI in analyzing the musculoskeletal system, it has been reported that MRI can be an accurate method to identify articular cartilage lesions[15,16,19,24,31] and the use of 7.0-T MRI has been reported to improve the contrast and resolution of articular cartilage over 3.0-T images.[4,11,18,28,30] In the present study, the medial joint compartment, in particular the medial tibial plateau, was evaluated because this region is where articular cartilage lesions due to posterolateral knee injuries have been reported to be the most severe.[17,22] Furthermore, previous studies using in vivo animal models of osteoarthritis in the knee have reported that early osteoarthritic changes were more significant on the tibial than the femoral side,[7,34] and it has been reported that in tibiofemoral arthritis, analyzing the tibial side alone is adequate.[10,33,34]

A previous study by Bolbos et al[7] compared high-field 7.0-T MRI and histology measurements of mean articular cartilage thickness of the medial tibial plateau in meniscectomized and control guinea-pig knee joints and demonstrated a correlation between the MRI and histomorphometric measurement techniques. In that study, however, MRI measurements were done in a sagittal plane, whereas the histologic measurements were done in a coronal plane. Our study, in which both MRI and histologic measurements were done in a coronal plane, determined that 7.0-T MRI and histology measurements of articular cartilage area in the medial tibial plateau in canines were correlated, but did not identify a significant correlation between maximum thickness measurements using these 2 techniques.

One limitation of our study was that it was difficult to determine that the MRI and histologic measurements were taken in exactly the same location and in parallel planes of section, although this potential error was minimized by comparing the MRI results with microradiographs of serially sectioned tibiae. We also recognize that some degree of tissue shrinkage occurs with routine fixation and processing methods; however, this would be expected to be consistent among samples because all were handled in the same way. It is known that the addition of cetylpyridinium chloride and cartilage fixation to the primary fixative results in improved retention of the proteoglycan content of the matrix and should be used for studies in which immunolocalization of proteoglycans is done[20]; however, this fixation technique was not used in this study. Finally, error in the thickness measurements may have occurred because of the potential lack of precision in determining the junction of uncalcified versus calcified cartilage on the MRI scans. However, the observed changes, which are assumed to be related to degeneration of cartilage, are statistically significant and consistent with previous reports on early osteoarthritis changes[3,25] despite the small sample size. Because this study was a preliminary analysis to determine if articular cartilage area and thickness measurements could be correlated between 7-T MRI and histology, future studies are planned with increased animals, and comparison with more conventional 1.5-T and 3.0-T MRI scanners.

In conclusion, we found that 7.0-T MRI scanning provides an alternative method to histology to evaluate articular cartilage area. This is important because the use of this technique will allow the potential detection of osteoarthritic changes in in vivo animal models without the need of euthanizing the animals for quantitative histologic analysis. This study also demonstrated that increases in articular cartilage thickness occur reproducibly in the operated knee of dogs using this surgical model. Whether these changes are followed by articular cartilage degeneration and fibrillation will require a longer-term study. The long-term goals of these studies will be to improve the monitoring of the natural history of early osteoarthritic changes or sequelae from knee injuries and to potentially evaluate the efficacy of osteoarthritis treatments.

ACKNOWLEDGMENT

This project was supported by the Sports Medicine Research Fund of the Minnesota Medical Foundation and National Institutes of Health grant BTRR–P41 RR008079.

REFERENCES

1. Adams ME. Cartilage hypertrophy following canine anterior cruciate ligament transaction differs among different areas of the joint. *J Rheumatol*. 1989;16(6):818-824.

2. Adams ME, Brandt KD. Hypertrophic repair of canine articular cartilage in osteoarthritis after anterior cruciate ligament transection. *J Rheumatol*. 1991;18(3):428-435.
3. Appleyard RC, Burkhardt D, Ghosh P, et al. Topographical analysis of the structural, biochemical and dynamic biomechanical properties of cartilage in an ovine model of osteoarthritis. *Osteoarthritis Cartilage*. 2003;11(1):65-77.
4. Banerjee S, Krug R, Carballido-Gamio J, et al. Rapid in vivo musculoskeletal MR with parallel imaging at 7T. *Magn Reson Med*. 2008; 59:655-660.
5. Behr B, Stadler J, Michaely HJ, Damert HG, Schneider W. MR imaging of the human hand and wrist at 7 T. *Skeletal Radiol*. 2009;38: 911-917.
6. Blumenkratz G, Majumdar S. Quantitative magnetic resonance imaging of articular cartilage in osteoarthritis. *Eur Cell Mater*. 2007;13: 76-86.
7. Bolbos R, Benoit-Cattin H, Langlois J-B, et al. Measurement of knee cartilage thickness using MRI: a reproducibility study in a meniscectomized guinea pig model of osteoarthritis. *NMR Biomed*. 2008; 21:366-375.
8. Calvo E, Palacios I, Delgado E, et al. High-resolution MRI detects cartilage swelling at the early stages of experimental osteoarthritis. *Osteoarthritis Cartilage*. 2001;9(5):463-472.
9. Chang G, Pakin SK, Schweitzer ME, Saha PK, Regatte RR. Adaptations in trabecular bone microarchitecture in Olympic athletes determined by 7T MRI. *J Magn Reson Imaging*. 2008;27(5):1089-1095.
10. Cicuttini FM, Wluka AE, Stuckey SL. Tibial and femoral cartilage changes in knee osteoarthritis. *Ann Rheum Dis*. 2001;60:977-980.
11. Eckstein F, Burstein D, Link T. Quantitative MRI of cartilage and bone: degenerative changes in osteoarthritis. *NMR Biomed*. 2006;19:822-854.
12. Fernandes JC, Martel-Pelletier J, Lascau-Coman V, et al. Collagenase-1 and collagenase-3 synthesis in normal and early experimental osteoarthritic canine cartilage: an immunohistochemical study. *J Rheumatol*. 1998;25(8):1585-1594.
13. Goldring MB, Goldring SR. Osteoarthritis. *J Cell Physiol*. 2007; 213:626-634.
14. Griffith CJ, LaPrade RF, Coobs BR, Olson EJ. Anatomy and biomechanics of the posterolateral aspect of the canine knee. *J Orthop Res*. 2007;25:1231-1242.
15. Guntern DV, Pfirrmann CW, Schmid MR, et al. Articular cartilage lesions of the glenohumeral joint: diagnostic effectiveness of MR arthrography and prevalence in patients with subacromial impingement syndrome. *Radiology*. 2003;226(1):165-170.
16. Jaremko JL, Maciejewski CM, Cheng RWT, et al. Accuracy and reliability of MRI vs. laboratory measurements in an ex vivo porcine model of arthritic cartilage loss. *J Magn Reson Imaging*. 2007; 26:992-1000.
17. Kannus P. Nonoperative treatment of grade II and III sprains of the lateral ligament compartment of the knee. *Am J Sports Med*. 1989; 17:83-88.
18. Krug R, Carballido-Gamio J, Banerjee S, et al. In vivo bone and cartilage MRI using fully-balanced steady-state free-precession at 7 Tesla. *Magn Reson Med*. 2007;58:1294-1298.
19. Kwack KS, Cho JH, Kim MS, et al. Comparison study of intraarticular and intravenous gadolinium-enhanced magnetic resonance imaging of cartilage in a canine model. *Acta Radiol*. 2008;49(1):65-74.
20. Landemore G, Quillec M, Oulhaj N, Izard J. Collage-associated sulphated proteoglycans: ultrastructure after formaldehyde—cetylpyridinium chloride fixation. *Histochem J*. 1991;23:534-540.
21. LaPrade RF, Wentorf FA, Crum JA. Assessment of healing of grade III posterolateral corner injuries: an in vivo model. *J Orthop Res*. 2004; 22:970-975.
22. LaPrade RF, Wentorf FA, Olson EJ, Carlson CS. An in vivo injury model of posterolateral knee instability. *Am J Sports Med*. 2006; 34:1313-1321.
23. Little CB, Ghosh P, Bellenger CR. Topographic variation in biglycan and decorin synthesis by articular cartilage in the early stages of osteoarthritis: an experimental study in sheep. *J Orthop Res*. 1996; 14(3):433-444.
24. Masi JN, Sell CA, Phan C, et al. Cartilage MR imaging at 3.0 versus that at 1.5T: preliminary results in a porcine model. *Radiology*. 2005;236(1):140-150.
25. McDevitt C, Gilgertson E, Muir H. An experimental model of osteoarthritis: early morphological and biochemical changes. *J Bone Joint Surg Br*. 1977;59(1):24-35.
26. Miosge N, Hartmann M, Maelicke C, Herken R. Expression of collagen type I and type II in consecutive stages of human osteoarthritis. *Histochem Cell Biol*. 2004;122(3):229-236.
27. Olson EJ, Wentorf FA, McNulty MA, Parker JB, Carlson CS, LaPrade RF. Assessment of a goat model of posterolateral knee instability. *J Orthop Res*. 2008;26:651-659.
28. Pakin SK, Cavalcanti C, La Rocca R, Schweitzer ME, Regatte RR. Ultra-high-field MRI of knee joint at 7.0T: preliminary experience. *Acad Radiol*. 2006;13:1135-1142.
29. Regatte RR, Schweitzer ME. Novel contrast mechanism at 3 Tesla and 7 Tesla. *Semin Musculoskel Radiol*. 2008;12:266-280.
30. Regatte RR, Schweitzer ME. Ultra-high-field MRI of the musculoskeletal system at 7.0T. *J Magn Reson Imaging*. 2007;25:262-269.
31. Saupe N, Pfirrmann CWA, Schmid MR, Schertler T, Manestar M, Weishaupt D. MR imaging of cartilage in cadaveric wrists: comparison between imaging at 1.5 and 3.0T and gross pathologic inspection. *Radiology*. 2007;243(1):180-187.
32. Vaughan JT, Snyder CJ, DelaBarre LJ, et al. Whole-body imaging at 7 T: preliminary results. *Magn Reson Med*. 2009;61(1):244-248.
33. Wachsmuth L, Keiffer R, Juretschke H, Raiss RX, Kimmig N, Lindhorst E. In vivo contrast-enhanced micro MR-imaging of experimental osteoarthritis in the rabbit knee joint at 7.1T. *Osteoarthritis Cartilage*. 2003;11(12):891-902.
34. Woo SLY, Gomez MA, Inoue M, Akeson WH. New experimental procedures to evaluate the biomechanical properties of healing canine medial collateral ligaments. *J Orthop Res*. 1987;5:425-432.